International Journal of Mass Spectrometry 218 (2002) 49–62

www.elsevier.com/locate/ijms

Comparative study of the binary clusters of acetic acid–water and acetic acid–benzene using electron impact and multiphoton ionization techniques

Y.B. Pithawalla[1] , C. Covington, I. McComish, I.N. Germanenko, M. Samy El-Shall*

Department of Chemistry, Virginia Commonwealth University, 23284-2006 Richmond, VA USA

Received 28 January 2002; accepted 2 April 2002

Abstract

Electron impact and multiphoton ionization techniques are used for a comparative study of the acetic acid–water and acetic acid–benzene clusters generated by supersonic beam expansion. In acetic acid–water clusters, hydrogen-bonding interaction is the driving force in determining the structures of the clusters. The protonated and the methyl cation containing clusters are characterized by 6-membered cyclic and 8-membered bicyclic structures. The similar magic number patterns observed for the protonated and methyl cation containing clusters suggest that the cyclic structures are stabilized by the charge interaction. A remarkable periodicity in the ion intensity of benzene (acetic acid)$_n$ clusters is observed. The clusters containing an even number of acetic acid molecules exhibit enhanced ion intensities. This effect is attributed to the formation of multiple cyclic dimers as a result of clustering from a dimer-rich vapor phase. Protonated acetic acid clusters are generated following the three-photon absorption by the binary clusters, which leads to dissociative charge transfer followed by proton transfer within the ionized acetic acid clusters. Evidence is presented for the special stability of the B_2A_8 ion, which is proposed to consist of a benzene dimer cation entrapped between two acetic acid tetramers. (Int J Mass Spectrom 218 (2002) 49–62) © 2002 Elsevier Science B.V. All rights reserved.

Keywords: Clusters; Acetic acid–water; Acetic acid–benzene; Multiphoton ionization; Cyclic dimers

---

1. Introduction

The study of molecular clusters and cluster ions is an active area of research in the rapidly advancing field of cluster science [1,2]. Of particular interest are the binary clusters composed of non-polar aromatics and polar or hydrogen bonded molecules. Examples of these systems include clusters of benzene with water [3], methanol [4] and acetonitrile [5] molecules. The studies of these systems are motivated by many concerns including fundamental understandings of solute–solvent interactions, energetics and dynamics of solvent evaporation as well as molecular level insights into some condensed phase processes such as microphase separation, miscibility gap, surface enrichment and binary nucleation.

Acetic acid molecules are known to form stable dimers in the gas phase and this process has been extensively studied for more than 50 years [6–13]. Due to the stability of the planar cyclic dimer involving

---

* Corresponding author. E-mail: selshall@hsc.vcu.edu

[1] Present address: Research, Development and Engineering Center, Philip Morris, Richmond, VA 23234, USA.

PII S1387-3806(02)00646-2

two hydrogen bonds ($\Delta H^\circ \approx -14$ kcal/mol, C_{2h} symmetry from electron diffraction studies [6,10]), it is generally assumed that the dimer is the only important associated species in the vapor phase of acetic acid [14]. Thus, the vapor is considered as an equilibrium mixture of monomers and cyclic dimers with no contributions from higher order clusters [10]. However, several reports have provided evidence for the existence of acetic acid polymers larger than dimers in the vapor phase [7,8,15,16]. Questions regarding the structures of higher order clusters and whether the liquid contains chain-like, hydrogen-bonded oligomers or cyclic and bicyclic structures remain unsolved [13,17–20].

The clusters of acetic acid (A) with water (W) and benzene (B) represent two interesting classes of binary clusters with different types of intermolecular interactions. Ionization of the $A_{n'}W_{m'}$ clusters results in the formation of the protonated clusters $H^+A_nW_m$ (with $n < n'$ and $m < m'$) where an extended hydrogen-bonding network reflects the dominant interaction among the cluster constituents. The formation of the ionic hydrogen bond with the tendency to build up an extended network is expected to interrupt the structure of the acetic acid dimers. On the other hand, because of the difference in the ionization potentials between benzene (9.2 eV) and acetic acid (10.6 eV [21]), ionization of the A_nB_m clusters will generate benzene ions surrounded by neutral acetic acid molecules or clusters. The resulting cluster ion distributions could provide information on some of the unique structures that might exist as a result of the ion–neutral interactions between benzene ions and different combinations of acetic acid molecules.

In order to gain a better understanding of the structures and formation mechanism of higher order acetic acid clusters, we have studied the binary clusters of acetic acid with water and benzene generated by supersonic beam expansions and ionized using electron impact (EI) or multiphoton ionization (MPI) techniques. Because of the high concentration of the acetic acid dimers in the vapor phase at room temperature (91% at 0.1 atm [13]), the pre-expansion vapor will be dominated by acetic acid dimers. It is, therefore, interesting to examine the effect of the pre-formed dimers on the distribution of cluster ions in both A_nW_m and the A_nB_m systems.

The organization of the paper is as follows. In the EI study, we investigate the acetic acid clusters generated in the presence of a trace amount of water in the pre-expansion vapor mixture. We compare these clusters with the acetic acid–benzene clusters generated from low and high concentrations of benzene in the pre-expansion vapor. In the EI study, all the clusters produced are ionized and no selectivity based on the cluster's composition is possible. In the MPI study, we use resonance enhanced MPI (REMPI) to selectively ionize the BA_n binary clusters at their specific resonance absorptions. In this case, the cluster ion distribution is mostly determined by the absorption features of the neutral clusters and the frequency of laser light used. We also use the non-resonance MPI at 248 and 266 nm to ionize the binary clusters non-selectively, where all the clusters containing benzene can be ionized with the same efficiency. This is achieved by taking advantage of the larger absorption cross section of benzene at 248 nm as compared to acetic acid and adjusting the laser power to only ionize benzene containing clusters. The application of different ionization techniques provides useful information on the origin of the enhanced ion intensity observed for certain clusters. Finally, we use molecular orbital calculations to obtain further information of the structures of some selected clusters.

2. Experimental

Benzene–acetic acid clusters are generated by pulsed adiabatic expansion in a supersonic cluster beam apparatus [22,23]. The essential elements of the apparatus are jet and beam chambers coupled to quadrupole and time-of-flight mass spectrometers. Fig. 1 illustrates the experimental set-up with the two mass spectrometers used in these experiments.

The binary clusters are formed in a He—seeded jet expansion, and probed as a skimmed cluster beam in collision-free high vacuum with a delay between synthesis and probe (i.e. the neutral beam flight time) on

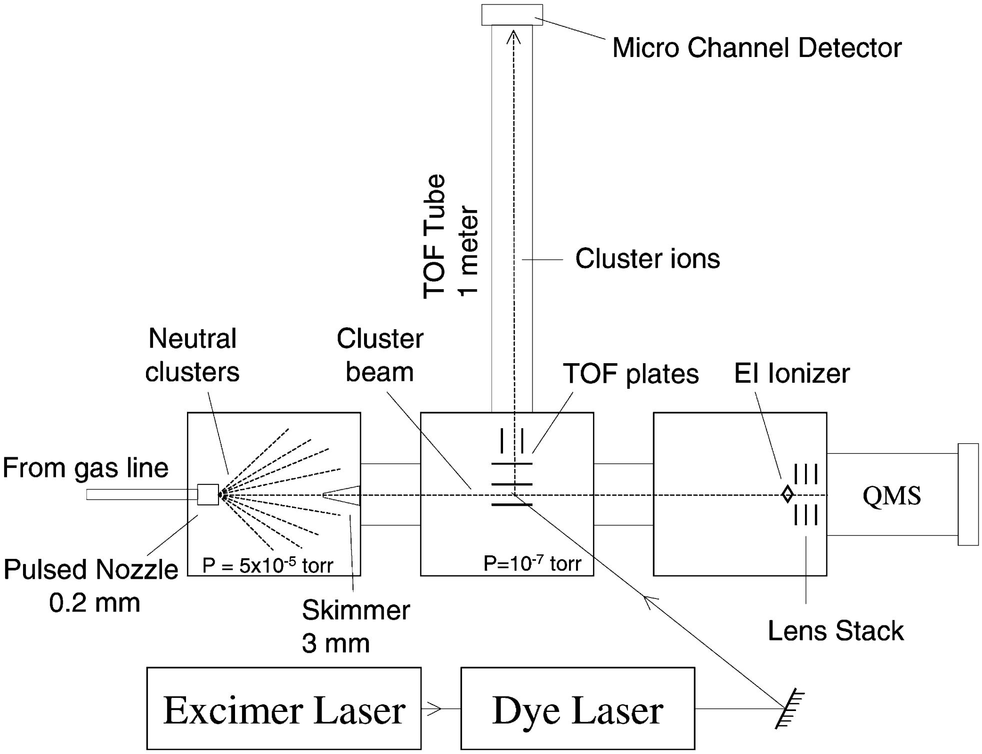

Fig. 1. Experimental set-up for the cluster beam time-of-flight and quadrupole mass spectrometers.

the order of 1 ms. During operation, a vapor mixture of benzene and acetic acid (Aldrich, 99.9% purity), in He (ultrahigh purity, Spectra Gases 99.999%) at a pressure of 2–8 atm is expanded through a conical nozzle (500 μm diameter) in pulses of 200–300 μs duration at repetition rates of 5–8 Hz. The jet is skimmed and passed into a high vacuum chamber, which is maintained at 8×10^{-8} to 2×10^{-7} Torr.

The cluster beam is ionized by using either MPI or EI. In the MPI experiments, the collimated cluster beam passes into the ionization region of a time-of-flight (TOF) mass spectrometer where it intersects a laser pulse from a frequency-doubled dye laser. The tunable radiation is provided by a dye laser (Lambda Physik FL3002) pumped by an excimer laser (Lambda Physik LPX-101). Coumarin 503 dye laser output passes through a β-BaB2O4 crystal (CSK Co.) cut at 65° to generate a continuously tunable frequency-doubled output of 10^{-8} s pulses. In other experiments, MPI of the binary clusters is achieved by either KrF (248 nm, power density $\approx 10^8$ W/cm^2) radiation provided by an excimer laser (Lumonics Hyper Ex-400) or by the fourth harmonic of a Nd:YAG laser (266 nm). The cluster ions formed by the MPI process are electrostatically accelerated in a two-stage acceleration region (300–400 V/cm), travel a field-free region (120 cm in length) to a two-stage microchannel-plate detector. Deflection plates are used to compensate for the cluster beam velocity. The deflection voltage is adjusted to optimize the signal for a particular mass range of interest. The TOF spectrum is recorded by digitizing the amplified current output of the detector by a 500 MHz digitizer (LeCroy 9350A) and averaged over 500–1000 pulses.

In the EI experiments, the cluster beam enters the ion source and quadrupole mass filter in an axial configuration. The mass spectrometer is an Extrel-4000 quadrupole equipped with 9.5-mm pole diameter rods.

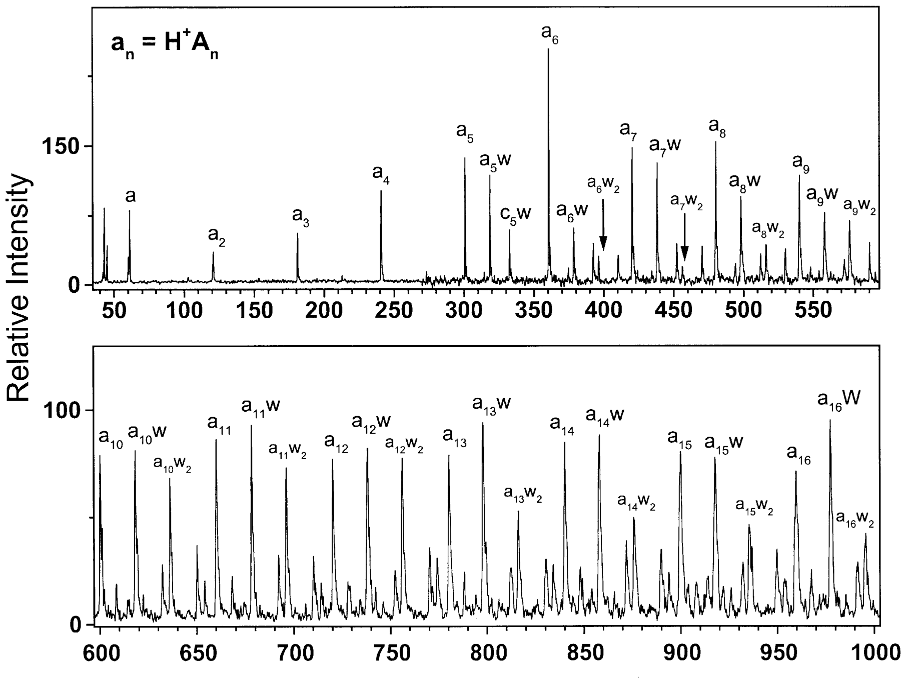
$a_n = H^+A_n$
Relative Intensity
0
150
100
Mass (amu)
50 100 150 200 250 300 350 400 450 500 550
600 650 700 750 800 850 900 950 1000
a
a_2
a_3
a_4
a_5
a_5W
c_5W
a_6
a_6W
a_6W_2
a_7
a_7W
a_7W_2
a_8
a_8W
a_8W_2
a_9
a_9W
a_9W_2
a_{10}
$a_{10}W$
$a_{10}W_2$
a_{11}
$a_{11}W$
$a_{11}W_2$
a_{12}
$a_{12}W$
$a_{12}W_2$
a_{13}
$a_{13}W$
$a_{13}W_2$
a_{14}
$a_{14}W$
$a_{14}W_2$
a_{15}
$a_{15}W$
$a_{15}W_2$
a_{16}
$a_{16}W$
$a_{16}W_2$

(a)

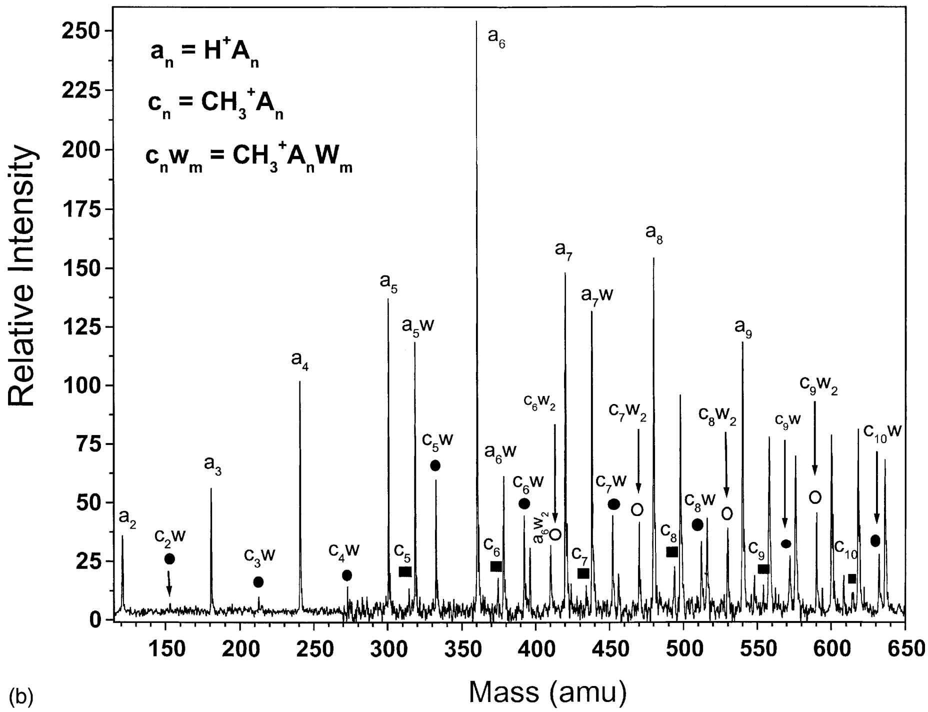
$a_n = H^+A_n$
$c_n = CH_3^+A_n$
$c_nW_m = CH_3^+A_nW_m$
Relative Intensity
0 25 50 75 100 125 150 175 200 225 250
Mass (amu)
150 200 250 300 350 400 450 500 550 600 650
a_2
c_2W
a_3
c_3W
a_4
c_4W
a_5
c_5
a_5W
c_5W
a_6
c_6
a_6W
c_6W
a_6W_2
c_6W_2
a_7
c_7
a_7W
c_7W
c_7W_2
a_8
c_8
c_8W
c_8W_2
a_9
c_9
c_9W
c_9W_2
c_{10}
$c_{10}W$

(b)

The amplified signal from the particle multiplier is processed using a boxcar integrator (EG&G model 166) set to sample at arrival times appropriate for the detected ions. At least 20 nozzle pulses per amu are averaged during each run.

3. Results and discussion

3.1. EI study of acetic acid–water clusters

Fig. 2(a) displays the quadrupole mass spectrum obtained following the 70 eV EI-ionization of the cluster beam produced from the supersonic expansion of acetic acid vapor in a He carrier gas containing a trace amount of water vapor (less than 1%). The most prominent cluster ion series are the protonated acetic acid series H^+A_n and the protonated acetic acid–water series $H^+A_nW_m$ with $n = 1–16$ and $m = 1–3$. In addition, two weak series of methyl ion solvated by acetic acid and acetic acid–water mixed clusters, $CH_3{}^+A_n$ and $CH_3{}^+A_nW_m$, are also present. These series are labeled C_n and C_nW_m, respectively as shown in Fig. 2(b). It is interesting to note that the retention of water in the protonated clusters starts when at least five acetic acid molecules are in the cluster (i.e. $n \geq 5$). The same behavior is also observed in the methyl ion series where the incorporation of the water starts to appear with the $CH_3{}^+A_5W$ cluster. The relative ion intensities of the H^+A_n series are higher than those of the $H^+A_nW_m$ series for $n \leq 10$. For larger acetic acid clusters with $n > 10$, the water containing clusters are enhanced and clusters incorporating two and three water molecules exhibit significant ion intensities.

The relative ion intensity plots of the observed cluster series are shown in Fig. 3. It is clear that the H^+A_n series exhibits a very pronounced peak at $n = 6$ and a less prominent peak at $n = 8$. A similar pattern is observed in the $CH_3{}^+A_n$ series, although the peak at $n = 8$ appears more pronounced relative to the $n = 6$ peak. On the other hand, the two most prominent peaks in the series containing one water molecule, H^+A_nW and $CH_3{}^+A_nW$, appear at $n = 5$ and 7 instead of 6 and 8. The enhanced abundances of the H^+A_5W and H^+A_6 are consistent with previous results obtained using a temperature- and pressure-variable EI source [24], and liquid ionization (LI) mass spectrometry [25,26].

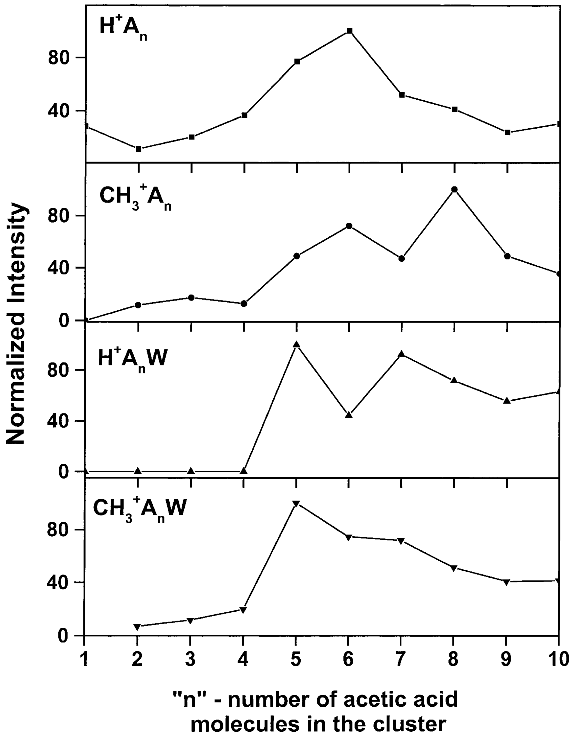

Fig. 3. Relative ion intensities of the cluster series H^+A_n, $CH_3{}^+A_n$, H^+WA_n, and $CH_3{}^+A_nW$ as functions of the number of acetic acid molecules in the cluster. Data corresponds to the EI spectra of Fig. 2.

The especially abundant ions (magic numbers) usually reflect some special stability related to structures of the cluster ions. The observation of the same magic

Fig. 2. (a) EI mass spectrum of protonated (acetic acid)$_n$, ($a_n = H^+A_n$) and protonated (acetic acid)$_n$(water)$_m$ (a_nw_m) clusters. The clusters are generated from the expansion of 15 Torr acetic acid vapor mixture in He, containing a trace amount of water vapor, at a total pressure of 1400 Torr. (b) EI mass spectrum of the methyl cation containing clusters $CH_3{}^+$(acetic acid)$_n$ labeled as c_n, and $CH_3{}^+$(acetic acid)$_n$(water)$_m$ labeled as c_nw_m. The expansion conditions are similar to those in (a).

numbers 6 and 8 in both the H^+A_n and $CH_3{}^+A_n$ series suggests that stable cyclic and bicyclic structures may be formed by the incorporation of 6 and 8 acetic acid molecules, respectively, in the cluster. Since the presence of a water molecule in the cluster shifts the magic numbers down by one less acetic acid molecule, it is suggested that water can substitute for acetic acid in the formation of the cyclic and bicyclic structures. The stability of the H^+A_5W ion has been attributed to a ring-type structure composed of five acetic acid molecules with a hydronium ion located in the center and slightly above the plane of the ring [24,25]. For the H^+A_6 ion, a similar ring structure could be formed with a protonated acetic acid molecule located in the center. Alternatively, 6-membered ring structures A_6 or A_5W attached to the proton or to the methyl cation could explain the stability of the H^+A_6 (or H^+A_5W) and the $CH_3{}^+A_6$ (or $CH_3{}^+A_5W$) ions.

3.2. *EI study of acetic acid–benzene clusters*

The major cluster ion series produced following the EI ionization of the supersonic beam containing a small concentration of benzene relative to acetic acid are $B_m{}^+A_n$ with $n = 1$–15 and $m = 1$–3. In addition, the protonated acetic acid series H^+A_n with $n = 1$–16 is also present. Fig. 4 displays a typical mass spectrum obtained following the EI ionization of the clusters produced from a pre-expansion mixture containing a 1:2 vapor ratio of benzene:acetic acid in a He carrier gas. Fig. 5 shows the variation in the relative ion intensity as a function of n (the number of acetic acid molecules in the cluster) for the $B_m{}^+A_n$ series with $m = 1$–3. In the B^+A_n series, a pronounced increase in the ion intensity is observed starting at $n = 4$. The $B_2{}^+A_n$ and $B_3{}^+A_n$ series exhibit clear even/odd alternation in the ion intensity, with the clusters containing

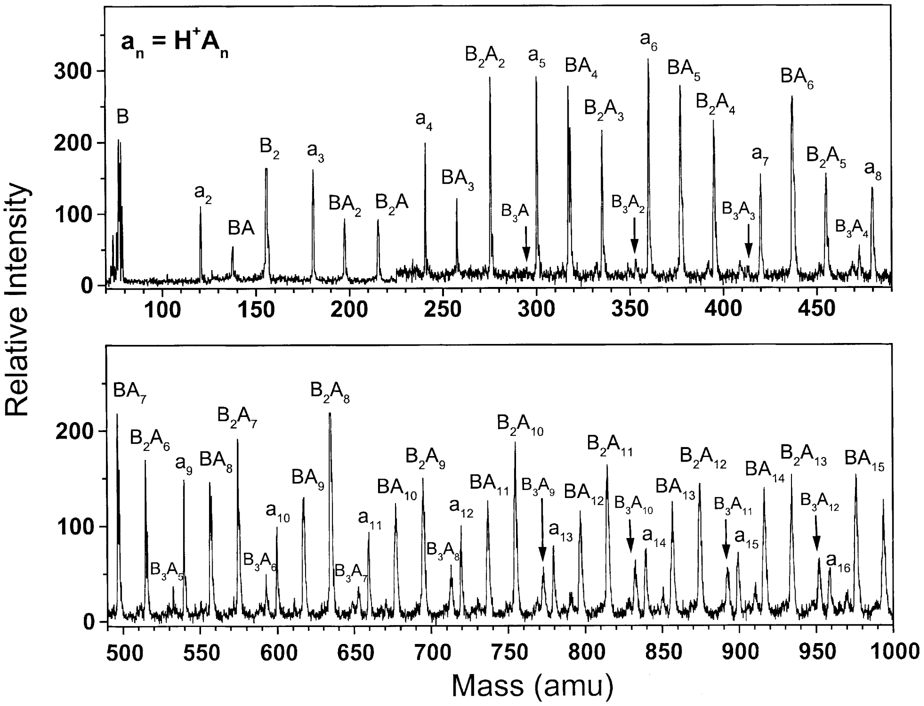

Fig. 4. EI mass spectrum of small $(\text{benzene})_m(\text{acetic acid})_n$ clusters (B_mA_n), The clusters are generated from the expansion of 7 Torr benzene and 15 Torr acetic acid vapor mixture in He at a total pressure of 1400 Torr.

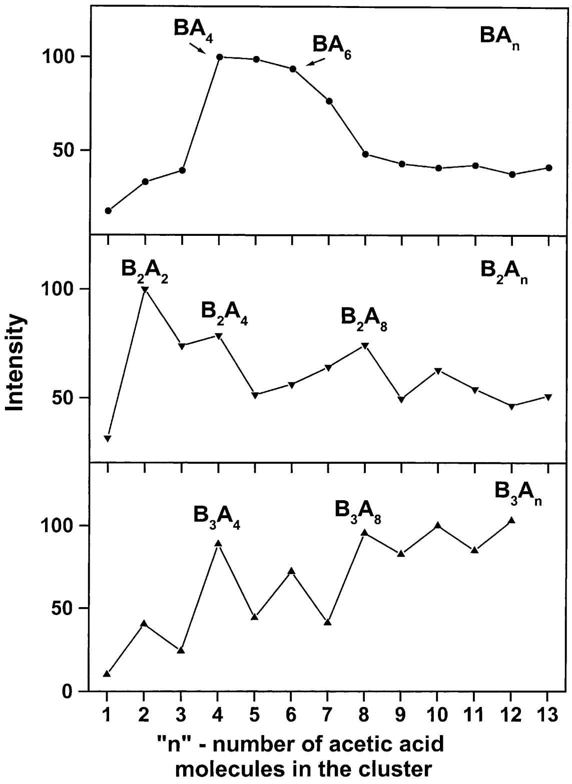

Fig. 5. Relative ion intensities of the cluster series B_mA_n for $m = 1–3$ as functions of the number of acetic acid molecules in the cluster. Data corresponds to the EI spectra of Fig. 4.

an even number of acetic acid molecules being the most abundant ions. By increasing the concentration of benzene in the pre-expansion vapor mixture, the cluster mass spectrum becomes dominated by benzene clusters (B_m, $m = 1–12$) and acetic acid clusters containing large number of benzene molecules ($B_m{}^+A_n$, $m = 1–11$ and $n = 1–10$). A typical example is shown in Fig. 6, which displays the mass spectrum obtained from the expansion of a vapor mixture containing a 2.7:1 ratio of benzene to acetic acid in a He carrier gas. Overall spectra of this type are found over a wide range of cluster composition B_nA_m, ranging from $n = 1$ to at least $n = 20$. The even/odd alternation is observed within clusters containing a larger number of benzene molecules in the series B_nA_m as shown in Fig. 7, which displays the variation of the relative cluster ion intensity with the number of acetic acid molecules in the cluster. The even/odd distribution will be further discussed with the results from the MPI study.

3.3. *MPI study of acetic acid–benzene clusters*

3.3.1. *REMPI results*

The absorption spectra of the BA_n clusters, with $n = 1–8$, relative to the 6^1_0 vibronic transition of the bare benzene molecule have been measured using resonant enhanced multiphoton ionization (REMPI). Well-defined spectral features were found for the BA_2, BA_3, BA_4, BA_6 and BA_8 clusters, and detailed spectroscopic results can be found in [27]. For the purpose of the present paper we only focus on the mass spectrometric results. Fig. 8 displays the mass spectrum obtained following the REMPI (at 259.26 nm) of the BA_n clusters generated from the expansion of a vapor mixture consisting of 0.01 Torr benzene, 58 Torr acetic acid in 6000 Torr He at 323 K. Under these conditions, the BA_n cluster series represents the most dominant species in the neutral cluster beam. The ion intensity within the BA_n series shows the same even/odd alternation observed in the EI study. A similar effect is also observed within the B_2A_n series as shown in the insert of Fig. 8.

The observation of a strong even/odd alternation in the integrated ion intensity within the absorption region of the BA_n clusters indicates that clustering of pre-formed dimers is the major association channel in the nucleation kinetics of supersaturated acetic acid vapor. The formation of BA_n clusters containing an even number of acetic acid molecules is therefore, a result of multiple associations of the hydrogen-bonded dimers. We assume that the presence of benzene does not change the clustering mechanism of acetic acid vapor. Benzene simply acts as a spectator for the acetic acid clusters via the measured perturbations in the benzene 6_0^1 transition induced by the acetic acid clusters [27].

The mass spectrum shows also the generation of the H^+A_n series. In all the MPI experiments, no ions could be generated in the absence of benzene in the beam expansion and no neat acetic acid clusters could

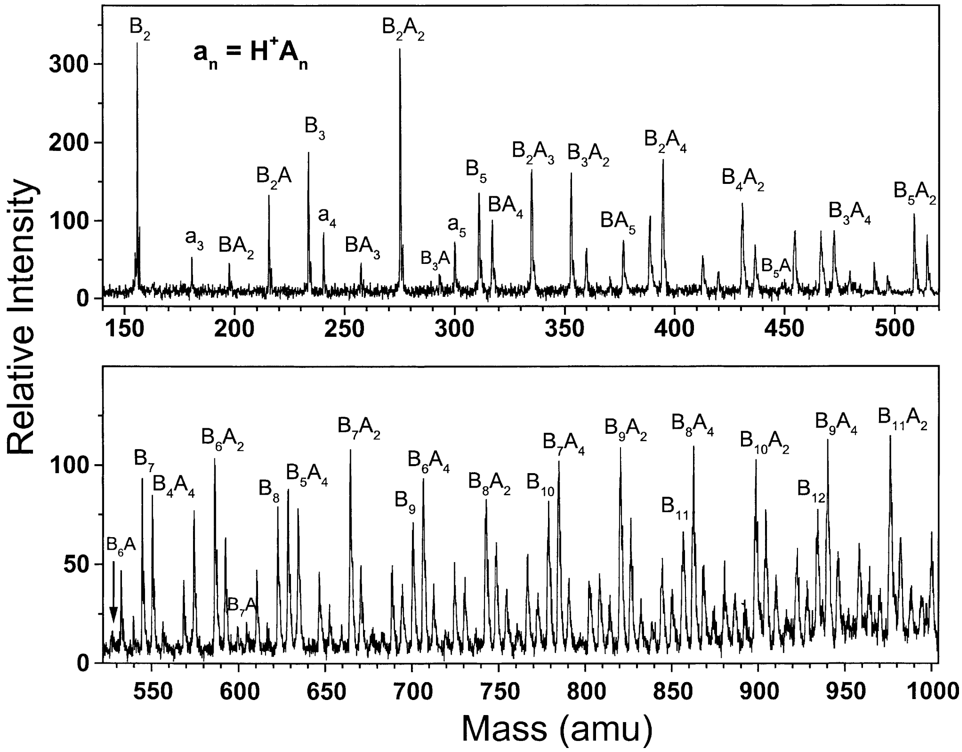

Fig. 6. EI mass spectrum of large (benzene)$_m$(acetic acid)$_n$ clusters (B_mA_n), showing the high abundance of the ions containing two and four acetic acid molecules. The clusters are generated from the expansion of 40 Torr benzene and 15 Torr acetic acid vapor mixture in He at a total pressure of 1400 Torr.

be ionized using the laser powers employed in the current experiments. This indicates that the H^+A_n ions are generated through intracluster dissociative charge transfer reactions, which produce ionized acetic acid clusters. The ionized acetic acid clusters $(CH_3COOH)_n{}^+$ then undergo the well-known proton transfer reaction to form the protonated series $H^+(CH_3COOH)_{n-1}$. Intracluster charge transfer from ground state $C_6H_6{}^+$ to acetic acid clusters A_n is only favorable if the IP of A_n is less than that of benzene (9.25 eV), which is only expected for very large A_n clusters. However, the observation of the protonated series H^+A_n starting from $n = 1$, suggests that charge transfers from electronically excited benzene ions are probably involved. We note that the generation of the first excited state of $C_6H_6{}^+$ ($\approx$2 eV above the ground state ion [28]) requires the absorption of more than two photons of the 266, 259 nm or the 248 nm laser lines used in the current experiments. In fact, the log, −log plot of the ion signal of the H^+A_n series vs. the laser power at 259 nm has a slope of 3.1 which indicates that the generation of the H^+A_n proceeds via the absorption of three photons by the binary neutral clusters.

3.3.2. MPI results

Fig. 9 displays the mass spectrum obtained following the MPI (at 248 nm) of the benzene–acetic acid clusters generated from the expansion of a vapor mixture consisting of 27 Torr benzene, 6 Torr acetic acid and 1300 Torr He at 295 K. Unlike the REMPI experiments where ionization is preceded by resonance absorption from different binary clusters at specific wavelengths, in the 248 nm ionization all the clusters containing benzene molecules are ionized with equal probability since these binary clusters do not exhibit resonance absorption at this wavelength.

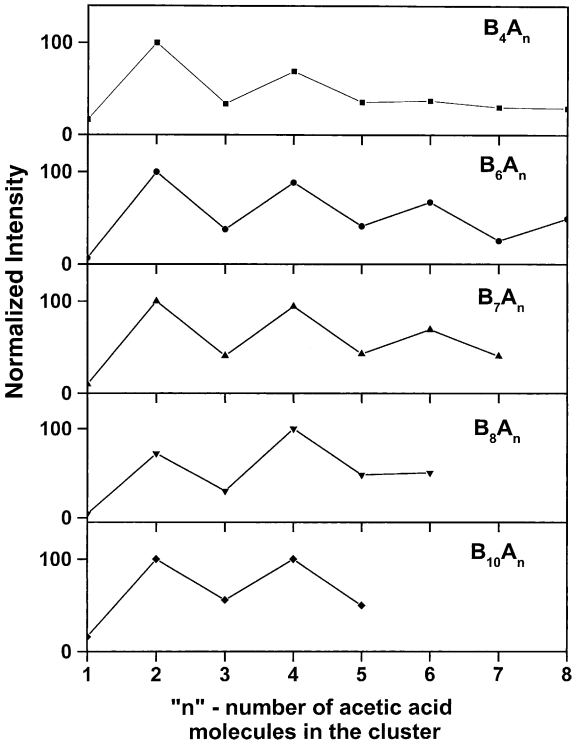

Fig. 7. Relative ion intensities of the cluster series B_mA_n for $m = 4$, 6–8 and 10 as functions of the number of acetic acid molecules in the cluster. Data corresponds to the EI spectra of Fig. 6.

By using a higher benzene concentration in the pre-expansion mixture, the abundance of clusters containing multiple benzene molecules can be enhanced as shown for the B_2A_n series. The ion intensity of this series shows unusual enhancement of the signal corresponding to the B_2A_8 ion (m/z 636). By using deutrated benzene (C_6D_6), instead of C_6H_6, the enhanced ion intensity is now observed at m/z 648 corresponding to $(C_6D_6)_2A_8$. This effect has been observed under the expansion conditions where the B_2A_n series is predominant independent of the method used for the ionization of the clusters.

The effect of different ionization methods on the observed local maximum of the B_2A_8 ion intensity is illustrated in Fig. 10(a), by comparing the relative ion intensity within the B_2A_n series obtained by MPI (266 nm) and EI methods. In both cases, the even/odd feature of the ion intensity distribution is evident together with the remarkable local maximum observed for the B_2A_8 ion. It should be noted that the even/odd alternation is also observed within other series of the binary clusters containing more benzene molecules. For example, the ion intensity pattern within the B_3A_n series exhibits strong even/odd alternation as shown in Fig. 10(b).

The above results provide strong evidence for the favorable production of multiple acetic acid dimers by supersonic expansion from the dimer-rich acetic acid vapor, and for the unusual abundance of the B_2A_8 ion. It should be noted that other examples of even/odd alternation in ion intensity have been reported and attributed to the alternating formation of cyclic and acyclic oligomer ions in ionized olefin systems [29,30]. A similar effect of intensity alternation has been observed for nitric oxide clusters and attributed to electronic effects derived from the pairing of electrons in the even-numbered clusters [31,32]. Recently, Miller and co-workers reported an interesting alternation in the ion intensity of $Fe^+(Ar)_n$ clusters, and explained the results by purely geometric effects which favor the even-numbered clusters [33].

3.4. Dimer and tetramer structures

It is interesting to speculate about the structures of the observed abundant ions. Ab initio calculations using the 6-31G** basis set predicts the well-known head-to-tail planar cyclic structure (I) to be a minimum energy structure of the acetic acid dimer (binding energy = −15.5 kcal/mol) [34]. In view of the stability of the cyclic dimer, a structure in which the benzene and the acetic acid dimer rings are stacked parallel to each other appears to be a reasonable candidate for the BA_2 cluster.

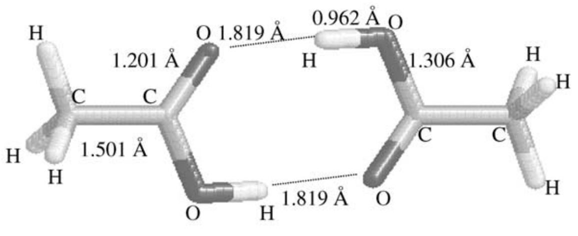

Structure (I) (6-31G**)

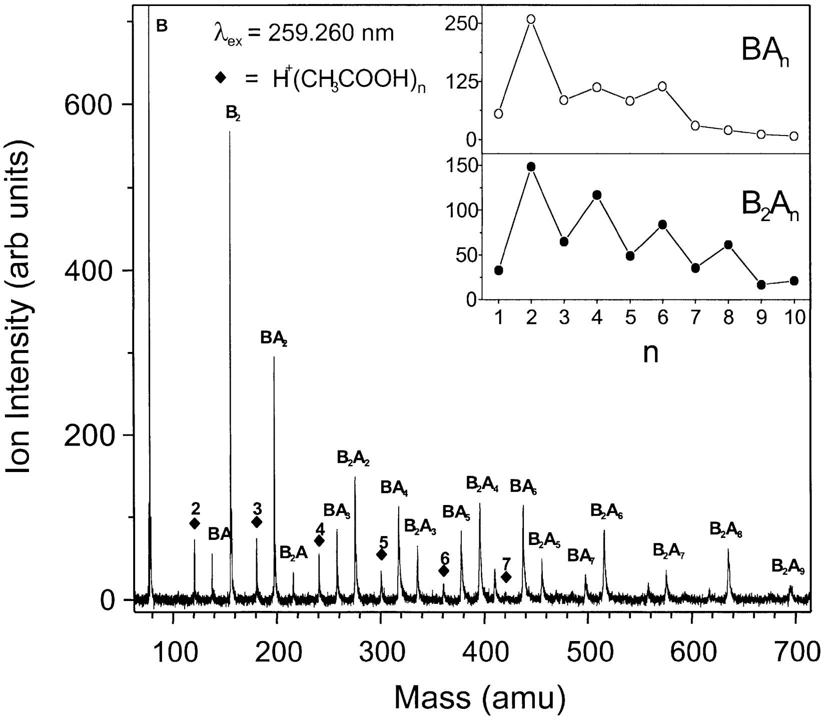

Fig. 8. REMPI mass spectrum of benzene–acetic acid clusters generated from the expansion of 0.01 Torr (194 K) benzene and 58 Torr (323 K) acetic acid vapor mixture in He at a total pressure of 6000 Torr, and $T = 323$ K. Insets show the relative abundance within the BA_n and B_2A_n series.

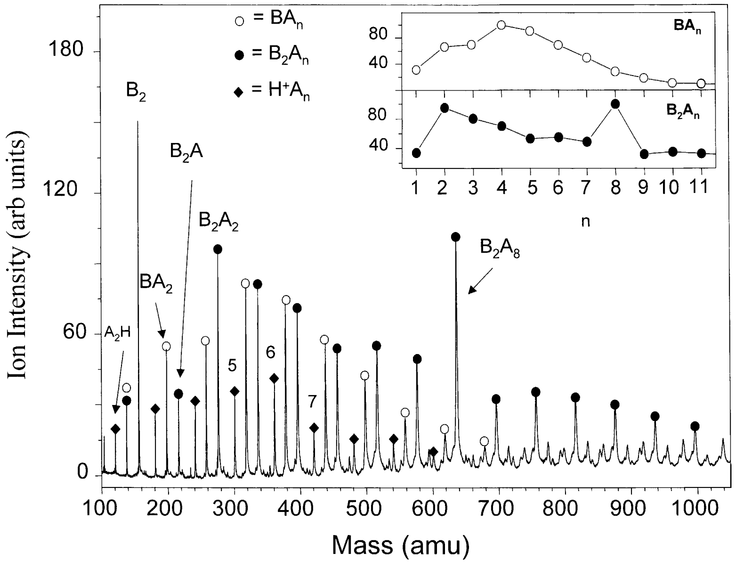

Fig. 9. MPI (at 248 nm) mass spectrum of benzene–acetic acid clusters generated from the expansion of 27 Torr (274 K) benzene and 6 Torr (282 K) acetic acid vapor mixture in He at a total pressure of 1300 Torr, and $T = 295$ K. Insets show the relative abundance within the BA_n and B_2A_n series.

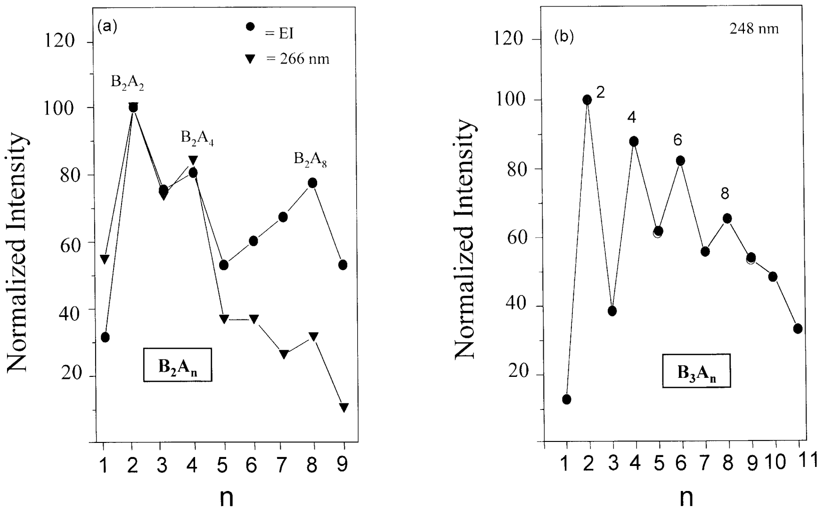

Fig. 10. (a) Relative ion intensity within the B_2A_n series obtained from EI and MPI (266 nm) ionization of the neutral cluster beam. In the EI experiment, the clusters are generated from the expansion of 80 Torr (295 K) benzene and 15 Torr (295 K) acetic acid vapor mixture in He at a total pressure of 1400 Torr, and $T = 295$ K. In the MPI experiment, the clusters are generated from the expansion of 700 Torr (350 K) benzene and 335 Torr (350 K) acetic acid vapor mixture in He at a total pressure of 2000 Torr, and $T = 350$ K. (b) Relative ion intensity within the B_3A_n series obtained from MPI (248 nm) ionization of the neutral cluster beam. The clusters are generated from the expansion of 27 Torr (274 K) benzene and 6 Torr (282 K) acetic acid vapor mixture in He at a total pressure of 1200 Torr, and $T = 295$ K.

The observation of alternation in the ion intensity of the binary B_mA_n clusters is consistent with structures containing multiple cyclic dimers of acetic acid around the benzene cluster ion. In addition, we propose the formation of a stable acetic acid tetramer in order to explain the observation of strong magic number for the B_2A_8 ion. Mori and Kitagawa [35] proposed a tetramer structure consisting of two dimers stacked in a staggered configuration, which avoids the steric interaction between the methyl groups. Castleman and co-workers, based on their electric deflection study of acetic acid clusters [36], proposed a trimer structure in which a third acetic acid molecule bridges across the dimer ring, i.e. the carbonyl group of the third acetic acid molecule is bridged to one of the hydrogens of the cyclic dimer, while the hydrogen from the OH of the monomer is bridged to a carbonyl group in the dimer structure (Fig. 4 in [36]). For the tetramer, they propose that the fourth acetic acid molecule adds to the trimer by another bridging structure across the opposite face of the cyclic dimer.

In order to evaluate the relative stability of the acetic acid tetramer as compared to two individual dimers, we carried out semi-empirical (AM1) calculations on the acetic acid tetramer starting from two dimers stacked in staggered (II) and eclipsed (III) configurations [34].

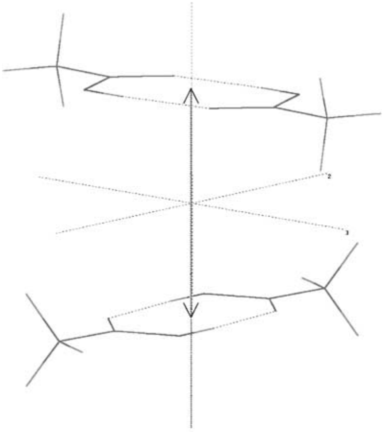

Structure II (AM1)
(E = -1.7 kcal/mol)

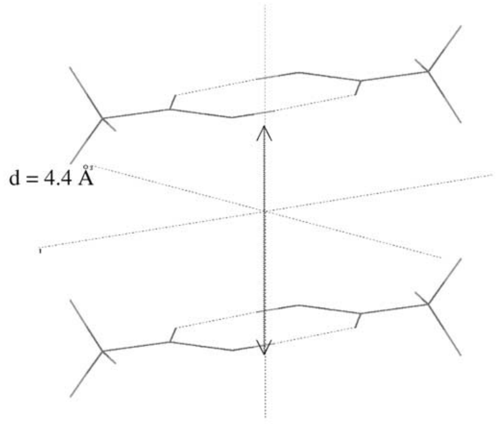

Structure III (AM1)
(E = 0.0)

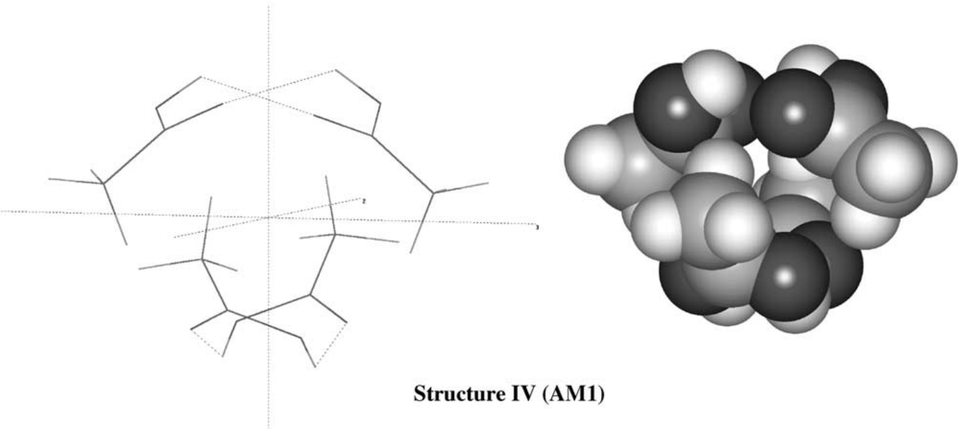

Structure IV (AM1)

The two staggered dimers (II) at the optimum interplanar distance of 4.4 Å gives a lower total energy (by 1.7 kcal/mol) than the two eclipsed dimers (III) at the same interplanar distance of 4.4 Å. (The eclipsed dimers did not result in a minimum in the total energy vs. interplanar distance plot.) However, full optimization of the staggered structure results in a lower energy structure (IV) where the two dimers are tilted from the planar configuration. Structure (IV) gives a total energy lower by 3.5 kcal/mol than the energy of two isolated dimers optimized at same level of calculations (AM1). The same trend was found from the ab initio calculation of structure (II) where geometry optimization at the 6-31 G** level results in structure (V), which is nearly similar to structure (IV). The main difference between structures (IV) and (V) is that in (V) the two dimer rings are less tilted inwards and appear to retain a higher degree of planarity as compared to structure (IV) (the dihedral angle C_2–$O_1 \cdots H$–O'_1 in structure (V) is 45.0°).

Our observation of a magic number behavior for the B_2A_8 ion but not for the BA_8 suggests that the benzene dimer cation is contributing to the stability of the B_2A_8 ion. Due to the contribution from charge transfer resonance interaction, the benzene dimer cation possesses a large binding energy (≈17 kcal/mol), as compared to other aromatic or mixed aromatic dimer cations

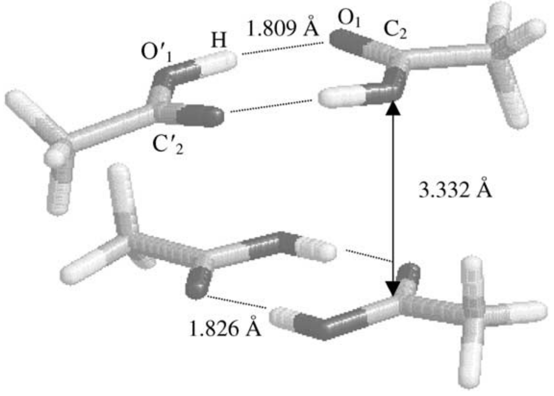

Structure (V) (6-31G)**

[37]. Also, the stacked structure is the most likely structure of B_2^+ since it maximizes the π-resonance interaction [38]. In view of these considerations, we propose a structure for the B_2A_8 ion, where the benzene dimer cation is placed between two acetic acid tetramers, each possessing a structure similar to (V). It should be noted that this proposed structure could also be an appropriate candidate for the neutral B_2A_8 cluster where the most stable structure of the benzene dimer is known to be the perpendicular configuration (T-shaped) [39]. However, recent calculations have shown that the difference in the binding energy between the T-shaped and parallel-displaced structures of the neutral benzene dimer is quite small (0.2–0.3 kcal/mol) [40]. This means that little change in the structure of the B_2A_8 neutral cluster could be expected upon the ionization of the benzene dimer unit, which is consistent with the observation of enhanced intensity of the B_2A_8 ion under different ionization methods.

4. Conclusions

In this paper, we have compared the nature of intermolecular interactions among acetic acid–water and acetic acid–benzene clusters. In the former case, hydrogen-bonding interaction is the driving force in determining the structures of the clusters. The protonated and the methyl cation containing clusters are characterized by 6-membered ring cyclic and 8-membered bicyclic structures. The similar magic number patterns observed for the protonated and methyl cation containing clusters suggest that the cyclic structures be stabilized by the charge interaction.

We have also examined the neutral acetic acid clusters by probing the ionized benzene–acetic acid binary clusters where the charge resides on the benzene moiety. A remarkable periodicity in the ion intensity is observed with clusters containing an even number of acetic acid molecules being more abundant. This effect is independent of the ionization method (REMPI at 259 nm, MPI at 248 nm, MPI at 266 nm and EI) indicating the generation of multiple dimers as a result of clustering from a dimer-rich vapor phase. Protonated acetic acid clusters are generated following the three-photon absorption by the binary clusters, which leads to dissociative charge transfer followed by proton transfer within the ionized acetic acid clusters. Evidence is presented for the special stability of the B_2A_8 ion, which is proposed to consist of a benzene dimer cation entrapped between two acetic acid tetramers.

Acknowledgements

The authors gratefully acknowledge financial support from NSF Grant no. CHE 9816536. Acknowledgment is also made to the donors of the Petroleum Research Fund, administered by the American Chemical Society for the partial support of this research.

References

[1] A.W. Castleman Jr., K.H. Bowen Jr., J. Phys. Chem. 100 (1996) 12911.
[2] A.W. Castleman Jr., S. Wei, Ann. Rev. Phys. Chem. 45 (1994) 685.
[3] R.N. Pribble, T.S. Zwier, Science 265 (1994) 75.
[4] A.W. Garrett, D.L. Severance, T.S. Zwier, J. Chem. Phys. 96 (1992) 7245.
[5] M.S. El-Shall, G.M. Daly, D.M. Wright, J. Chem. Phys., in press.
[6] J. Karle, L.O. Brockway, J. Am. Chem. Soc. 66 (1944) 574.
[7] H.L. Ritter, J.H. Simons, J. Am. Chem. Soc. 67 (1945) 757.
[8] E.W. Johnson, L.K. Nash, J. Am. Chem. Soc. 72 (1950) 548.
[9] D.M. Mathews, R.W. Sheets, J. Chem. Soc. A (1969) 2203.
[10] J.L. Derissen, J. Mol. Struct. 7 (1971) 81.
[11] T. Hagler, P. Dauber, S. Lifson, J. Am. Chem. Soc. 101 (1979) 5131.
[12] D.J. Frurip, L.A. Curtiss, M. Blander, J. Am. Chem. Soc. 102 (1980) 2610.
[13] J. Chao, B.J. Zwolinski, J. Phys. Chem. Ref. Data 7 (1978) 363.
[14] M.D. Taylor, J. Am. Chem. Soc. 73 (1951) 315.
[15] A.E. Potter, P. Bender, H.L. Ritter, J. Phys. Chem. 59 (1955) 250.
[16] L.E. Kolysko, E.Y. Gorodinskaya, Russ. J. Phys. Chem. 47 (1973) 737.
[17] K.D. Cook, J.W. Taylor, Int. J. Mass Spectrom. Ion Phys. 35 (1980) 259.
[18] H. Bertagnolli, Chem. Phys. Lett. 93 (1982) 287.
[19] M. Faubel, T. Kisters, Nature 339 (1989) 527.

[20] C.F. Wilcox, S.H. Bauer, J. Chem. Phys. 107 (1997) 5794.

[21] R.D. Levin, S.G. Lias, Ionization potential and appearance potential measurements, 1971–1981, National Bureau of Standards, 1982.

[22] M.S. El-Shall, Z. Yu, J. Am. Chem. Soc. 118 (1996) 13058.

[23] M.S. El-Shall, C. Marks, L.W. Sieck, M. Meot-Ner, J. Phys. Chem. 96 (1992) 2045.

[24] C. Lifshitz, W.Y. Feng, Inter. J. Mass Spectrom. Ion Processes 146 (1995) 223.

[25] M. Tsuchiya, S. Teshima, T. Kaneko, T. Hirano, J. Chem. Soc. Jpn. 6 (1993) 6867.

[26] A. Wakisaka, Y. Yamamoto, J. Chem. Soc. Chem. Commun. (1994) 2105;
A. Wakisaka, S. Takahashi, N. Nishi, J. Chem. Soc. Faraday Trans. 91 (1995) 4063.

[27] I.N. Germanenko, M.S. El-Shall, J. Phys. Chem. 103 (1999) 5847.

[28] H.M. Rosenstock, K.E. McColloh, F.P. Lossing, Int. J. Mass Spectrom. Ion Phys. 25 (1977) 309.

[29] V. Baranov, J. Wang, G. Javahery, S. Petrie, A.C. Hopkinson, D.K. Bohme, J. Am. Chem. Soc. 119 (1997) 2040.

[30] Y.B. Pithawalla, J. Gao, Z. Yu, M.S. El-Shall, Macromolecules 29 (1996) 8558.

[31] S.R. Desai, C.S. Feigerle, J.C. Miller, J. Chem. Phys. 101 (1994) 4526.

[32] H.S. Carman Jr., J. Chem. Phys. 100 (1994) 2629.

[33] S. Bililign, C.S. Feigerle, J.C. Miller, M. Velegrakis, J. Chem. Phys. 108 (1998) 6312.

[34] HyperChem(TM), Hypercube, Inc., Gainesville, Florida 32601, USA.

[35] Y. Mori, T. Kitagawa, Inter. J. Mass Spectrom. Ion Processes 84 (1988) 319.

[36] R. Sievert, I. Cadez, J. Van Doren, A.W. Castleman Jr., J. Phys. Chem. 88 (1984) 4502.

[37] K. Hiraoka, S. Fujimaki, K. Argua, J. Chem. Phys. 95 (1991) 8413.

[38] J.R. Grover, E.A. Walters, E.T. Hui, J. Phys. Chem. 91 (1987) 3233.

[39] H. Krause, B. Ernstberger, H.J. Neusser, Chem. Phys. Lett. 184 (1991) 411.

[40] P. Hobza, H.L. Selzem, E.W. Schlag, J. Phys. Chem. 100 (1996) 18790.